

The status of zaratite: investigation of the type specimen from Cape Ortegal, Galicia, Spain

JAVIER GARCIA-GUINEA^{1,*}, ANGEL LA IGLESIA², ELENA CRESPO-FEO³, JOSÉ GONZÁLEZ DEL TÁNAGO⁴ and VIRGILIO CORRECHER⁵

¹ Museo Nacional de Ciencias Naturales (MNCN-CSIC), C/José Gutiérrez Abascal 2, 28006 Madrid, Spain

*Corresponding author, e-mail: Javier.Garcia.Guinea@csic.es

² Instituto de Geociencias (CSIC, UCM), C/José Antonio Nováis 2, 28040 Madrid, Spain

³ Dept. Cristalografía y Mineralogía, Fac. Ciencias Geológicas Univ., Complutense de Madrid C/José Antonio Nováis 2, 28040 Madrid, Spain

⁴ Dept. Petrología y Geoquímica, Fac. Ciencias Geológicas Univ., Complutense de Madrid, C/José Antonio Nováis 2, 28040 Madrid, Spain

⁵ CIEMAT, Departamento Dosimetría Radiaciones, Avenida Complutense 22, 28040 Madrid, Spain

Abstract: Three zaratite samples from Cape Ortegal (type locality, Spain), Texas, Lancaster County (Pennsylvania) and Heazlewood (Tasmania) were analyzed by electron-probe micro-analysis (EPMA), environmental scanning electron microscopy with energy-dispersive spectrometer (ESEM-EDS), X-ray diffraction (XRD), differential thermal analysis and thermogravimetry (DTA-TG), micro-Raman and Fourier-transform infrared spectrometry (FTIR). The empirical formulae calculated from EPMA exhibit different molar ratios (Ni/CO₃, Ni/OH and H₂O/Ni), showing that these three samples referred to as ‘zaratite’ are chemically distinct; they are actually close to either anhydrous zaratite (Ortegal), nullaginite (Tasmania) or gaspéite (Pennsylvania). The XRD patterns of the three samples only validate their low-crystallinity character with variable mineral inclusions. Raman and FTIR spectra confirm large similarities among the three samples, in line with the general chemical kinship of these nickel hydroxycarbonate (\pm hydrate) materials. Our data suggest that the natural nickel hydroxycarbonate materials, collectively referred to as ‘zaratite’ on the basis of colour, occurrence and poor crystallinity, are in fact so diverse in terms of Ni/C/H ratios that the ‘zaratite’ term should not deserve a species status and so remains highly questionable.

Key-words: zaratite, Cape Ortegal (Galicia, Spain), Pennsylvania, Heazlewood, nickel hydroxycarbonate hydrate, Raman, FTIR, DTA-TG.

1. Introduction

Zaratite is one of those grand-fathered, but long-questioned, minerals because of its apparent near-amorphous nature and the difficulty in obtaining type material for investigation. Its characterization has been rendered difficult by its poorly crystalline structure, unstable hydration states, variable impurities and extremely scarce material useful for destructive analyses. The type specimen of zaratite from Cape Ortegal is classified by the International Mineralogical Association (IMA) with the status Q (questionable) due to the lack of a detailed characterization. The nickel carbonate hydroxide hydrate from Ortegal Cape studied by Casares in 1845 was firstly defined as the type mineral zaratite in a paper of Martínez Alcibar (1850). The chemical characterization of the mineral was very brief: acid dissolution with effervescence, blue coloration of the dissolution when adding ammonium hydroxide, particles

of metallic nickel in the reducing flame and copious yield of water in the closed tube, deducing that: “the chemical composition of the mineral is nickel carbonate hydrated similar to the artificial product analyzed by Berthier of composition: 47.5 protoxide of nickel, 14.0 carbonic acid and 38.5 per cent of water”. Smith & Brush (1853) provided the first, and the nowadays accepted, zaratite formula Ni₃CO₃(OH)₄·4H₂O on the basis of chemical analyses performed on the “*emerald of nickel*” of Pennsylvania (USA). Isaacs (1963) performed new chemical analyses on zaratite specimens from different deposits, which displayed some variations: NiO from 56.9 to 61.2; CO₂ from 13.5 to 15.7; H₂O from 23.2 to 27.1 wt%. Nevertheless, no further agreement exists on a chemical composition for zaratite. A similar situation can be observed in the published literature on the structural characterization of zaratite by X-ray diffraction methods, explained probably by its low crystallinity together with

the impurities variability. The first XRD data were provided by Fenoglio (1934) studying zaratite samples from Lancaster County, Pennsylvania, and Lilaz, Valle d'Aosta, Italy, providing a cubic cell with $a_0 = 6.35 \text{ \AA}$ compatible with the observed mineral isotropy. In the 50s, additional zaratite samples from Heazlewood (Tasmania), and Lancaster County (Pennsylvania) showed similar chemical composition and unclear XRD patterns, which could not be indexed with the previous cubic cell attributed to zaratite (Williams *et al.*, 1959). In the 60s, zaratite specimens from Pennsylvania and Heazlewood provided similar fuzzy XRD patterns with no possible indexation (Isaacs, 1963). These data on zaratite are included in the JCPDS File 16-0164 but no useful chemical and structural data were published later. Conversely, other research continued analyzing both natural zaratite and synthetic hydrous basic nickel carbonates using thermo-gravimetric (TG) and spectroscopic (Raman, FTIR) techniques to determine more accurately hydroxyl groups and molecular water in the zaratite formula. Particularly useful are the TG recordings at rising temperature and the kinetics studies on the decomposition of the synthetic nickel (II) carbonate hydroxide tetra-hydrate phase (*e.g.*, Henmi *et al.*, 1986; Fried & Dollimore, 1994; Shaheen, 2002; Rhamdhani *et al.*, 2008). Recent studies by Raman, IR, UV-Vis-NIR spectroscopy on Heazlewood zaratite (Frost *et al.*, 2008; Frost *et al.*, 2010) provide spectra to be compared with those obtained in this study on the zaratite type-specimen from Cape Ortegá. Unfortunately, in characterizing this type of material several difficulties arise: (i) the low crystallinity; (ii) the possibility that the hydration state depends on the environmental conditions, *e.g.* those of the type-locality (the wet cliffs of Cape Ortegá) differing from those of a long museum storage; the zaratite hydrous sample, 160 years ago, nowadays could reasonably be an anhydrous material [a similar case was observed in other nickel carbonates, *e.g.*, hellyerite $\text{NiCO}_3 \cdot 6\text{H}_2\text{O}$, which is relatively unstable and must be kept in an air-tight environment (Williams *et al.*, 1959; Anderson *et al.*, 2002)]; (iii) shortage in the amount of type specimen. These problems can be circumvented by using non-destructive molecular and chemical probes coupled to optical and electronic microscopes. With this aim, we performed in this study non-destructive and micro-destructive analyses of green particles taken from the Spanish historical sample by EPMA, ESEM-EDS, XRD, DTA-TG, micro-Raman and micro-FTIR. Additional analyses were also carried out on zaratite specimens from Texas (Lancaster County, Pennsylvania) and Heazlewood (Tasmania, Australia) for comparison purposes.

2. Samples and experimental methods

Nowadays, only two zaratite samples from Cape Ortegá are known. They are kept in Museo de Historia Natural Luis Iglesias (Santiago de Compostela) (photograph in Fig. 1a) and Museo Nacional de Ciencias Naturales (Madrid)

(photograph in Fig. 2a). We here studied the specimen Zaratite-E-1 stored in Madrid; it weighted 227.63 g with a size of $7 \times 6 \times 3 \text{ cm}^3$. Zaratite forms only a thin patina of green-emerald colour on a magnetite-hematite metallic mass and cannot be scratched without producing deterioration. The zaratite sample from Texas, Lancaster County (Pennsylvania) is a historical specimen stored in the Museo Nacional de Ciencias Naturales (Madrid) (probably since 1850), $9 \times 6 \times 2 \text{ cm}^3$ in size and weighting 310 g. The Tasmanian zaratite specimen from Heazlewood was bought from Adam's Minerals, with an original size of $3 \times 2 \times 0.5 \text{ cm}^3$ and a weight of 13 g.

Little particles taken from samples were scattered on a self-adhesive flat surface to be embedded in epoxy resin for the classic EPMA round-mount performance. The resultant polished surface displayed translucent micrograins with green-emerald appearance attributable to nearly pure zaratite together with other guest minerals with different aspect, such as magnesite, spinel, *etc.* Wavelength-dispersive electron-microprobe data for zaratite and associated minerals were collected using a Jeol JXA-8900M instrument. Standard operating conditions were: acceleration voltage 20 kV, probe current 50 nA, peak counting time 10 s and background counting time of 5 s, with a beam diameter of 2 to 5 μm . The standards used were garnet ($\text{MnK}\alpha$, $\text{FeK}\alpha$), albite ($\text{NaK}\alpha$, $\text{AlK}\alpha$), sillimanite ($\text{SiK}\alpha$), apatite ($\text{CaK}\alpha$, $\text{ClK}\alpha$), nickel ($\text{NiK}\alpha$), galena ($\text{SK}\alpha$), cobalt ($\text{CoK}\alpha$), copper ($\text{CuK}\alpha$), and chromium ($\text{CrK}\alpha$). Carbon was analyzed after gold coating and using an LDE2 crystal (acceleration voltage 15 kV, probe current 20 nA, 10 μm beam, and scapolite [$\text{CK}\alpha$] standard). The results were processed using an on-line ZAF program.

In addition, in the case of the zaratite from Cape Ortegá, the whole specimen was placed in the large chamber of an environmental scanning electron microscope (ESEM-EDS; FEI Inspect Company) where photomicrographs and EDS microanalyses were obtained.

The X-ray diffraction study of powdered zaratite was performed using Xpovder software, which allows a full duplex control of the Phillips PW 1730/00 diffractometer (Bragg-Brentano geometry) with $\text{Cu K}\alpha_{1-2}$ radiation, a Ni filter and a setting of 45 kV and 40 mA. The XRD patterns were obtained by continuous scanning from 3 to $60^\circ 2\theta$, with a receiving slit of 0.1 mm, $0.010^\circ (2\theta)$ step size and a recording time per step of 2 s. Given the sample scarcity, the zaratite powder was pressed onto a silicon oriented sample holder.

Thermo-gravimetric and differential thermal analysis (TG-DTA) of 5 mg of zaratite powder were recorded with a simultaneous TG-DTA-DSC Setaram thermal analyzer, Labsys CS 32-CS 332 Controller also in N_2 . Thermal treatments were performed with a heating rate of $10 \text{ }^\circ\text{C}\cdot\text{min}^{-1}$ from room temperature up to $1000 \text{ }^\circ\text{C}$. The sample was packed in an alumina crucible, and the reference material was an empty alumina crucible.

The micro-Raman spectra of zaratite micro-grains were measured in a Thermo-Fischer DXR Raman Microscope which has a point-and-shoot Raman capability of one micrometre spatial resolution. We used the $100\times$ objective

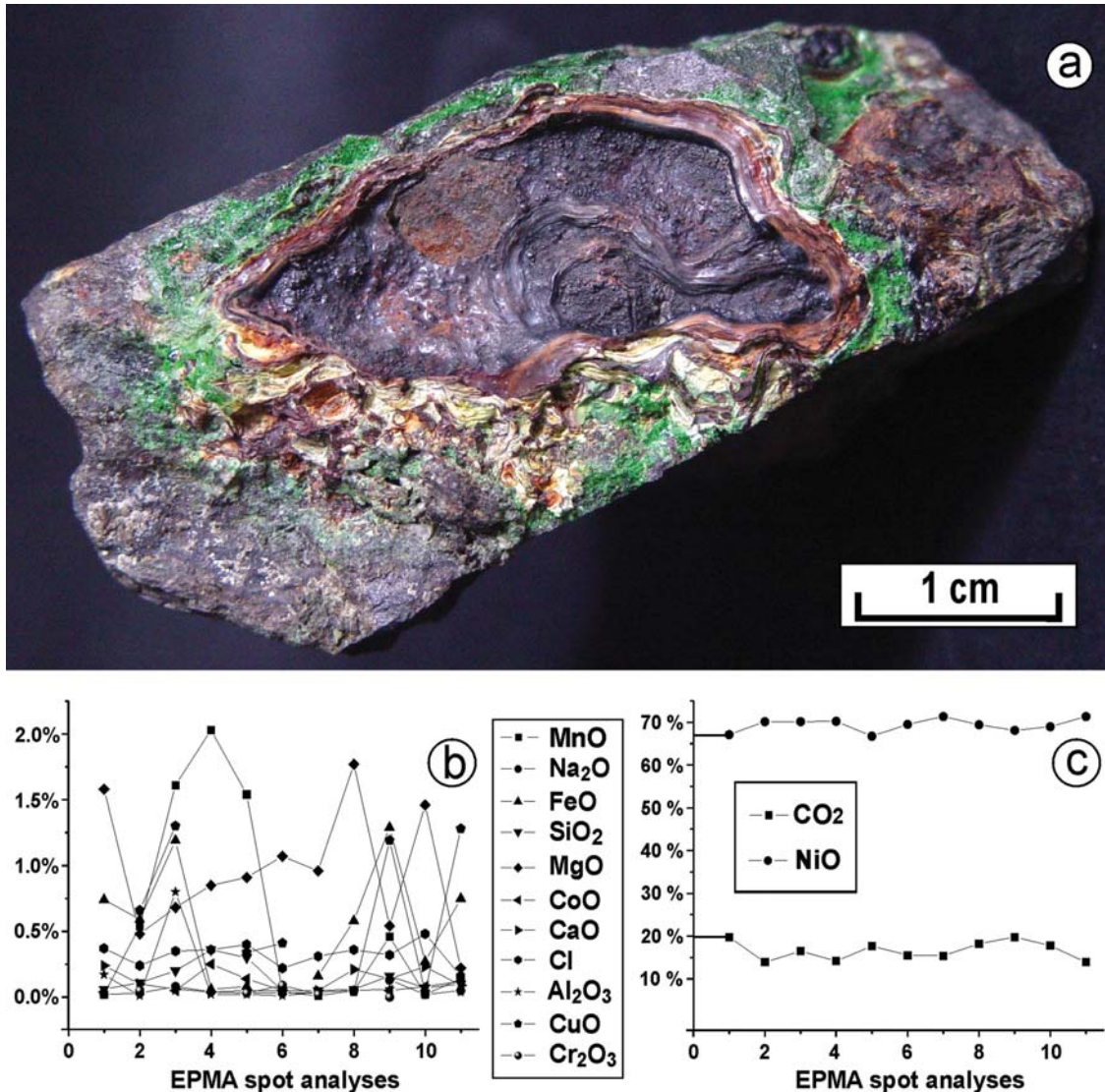


Fig. 1. (a) Photograph of the zaratite type specimen from Cape Ortegal (Spain) collected in 1850, stored in the Luis Iglesias Museum (Santiago de Compostela, Spain). (b) EPMA on zaratite areas and micro-particles; plot of the minor elements of the 11 EPMA analyses (MNCN Madrid sample). (c) Comparative plot of the major CO₂ and NiO components of 11 EPMA analyses (MNCN Madrid sample).

of the confocal microscope together with a 532 nm laser source delivering 10 mW at 100 % laser power mode. The average spectral resolution in the Raman shift ranging from 100 to 3600 cm⁻¹ was 4 cm⁻¹, with 900 lines/mm grating and 2 μm spot size. The system was operated under OMNIC 1.0 software fitting working conditions such as pinhole aperture of 25 μm, bleaching time 30 s; average of four exposures timed 10 s each.

The FT-IR spectra of green-translucent particles of zaratite were recorded in a Thermo Scientific Nicolet iN10 FT-IR microscope coupled to a Nicolet iZ10 FT-IR module, which has the ability to measure samples a few micrometres in size. Zaratite particles were measured with a slide-on germanium Tip-ATR crystal of high sensitivity specific for small particles. Spectra were collected in 8 seconds using OMNIC 1.0 software which combines infrared microanalysis and spectral identification.

3. Analytical results

3.1. Electron-probe micro-analyses

Table 1 and Fig. 1b and c exhibit a selection of eleven EPMA spot analyses of the cleanest zaratite masses from Cape Ortegal type material, previously selected under the optical microscope on the basis of their *emerald* resemblance. The analyses show NiO in the range of 65 to 71 wt% and CO₂ from 15 to 20 wt%, with totals between 98–95 wt%. Figure 1c highlights the major CO₂ and NiO contents and Fig. 1b the minor elements S, Mn, Na, Fe, Si, Mg, Co, Ca, Cl and Cu associated with the basic rock parageneses of the Cape Ortegal region. The zaratite formulae derived from the EMPA analyses were calculated with the following assumptions: (i) the water contents were stated by difference of the experimental totals to 100 wt%,

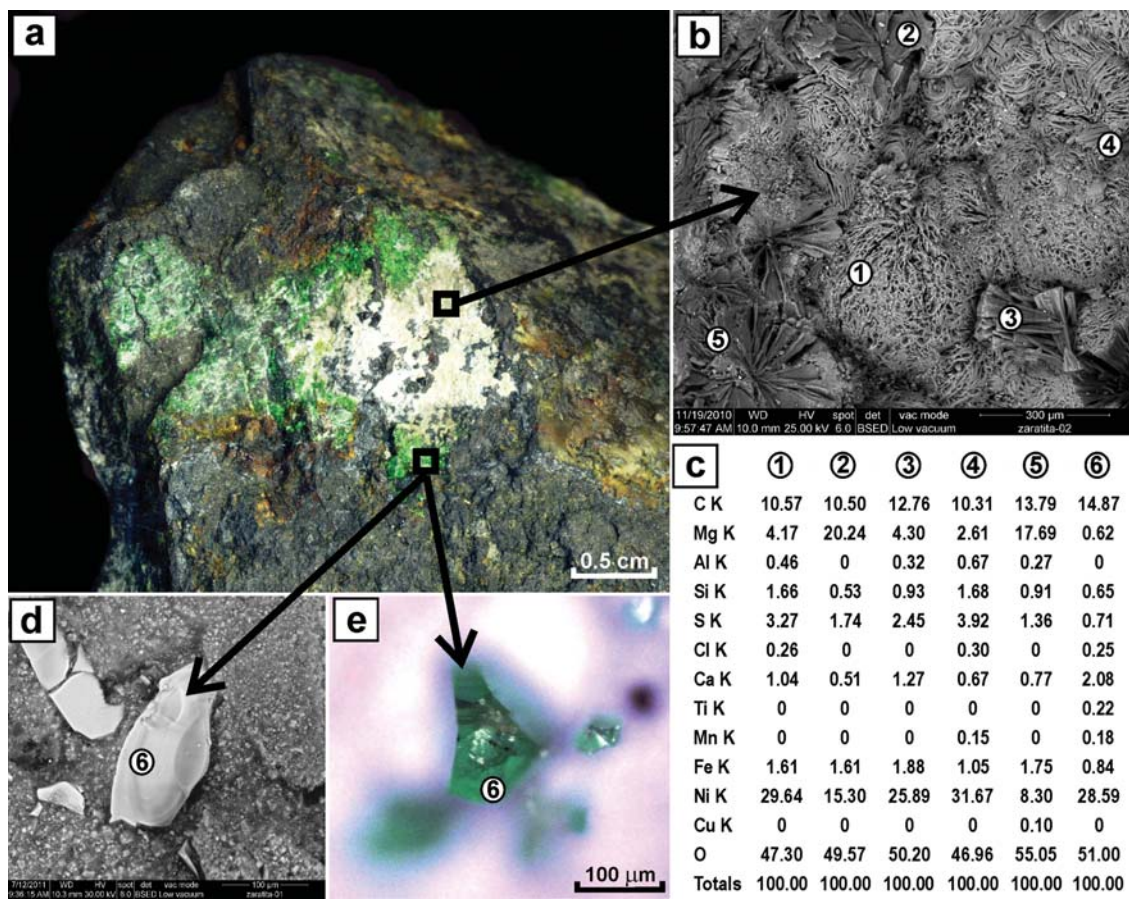


Fig. 2. Type specimen of zaraitite from Cape Ortegale (Spain; MNCN Madrid sample): (a) Sample in the ESEM chamber showing the analyzed areas, (b) backscattered-electron image with spot analyses positions, (c) table of the EDS spot analyses, (d) backscattered-electron image of a separated green pure zaraitite fragment, (e) photomicrograph of a zaraitite fragment taken in the DXR Raman microscope.

Table 1. EPMA on zaraitite fragments and spots taken on the dark green areas of the type specimen from Cape Ortegale (Coruña, Spain).

EPMA of the type specimen of zaraitite from Cape Ortegale (Spain)												
	1	2	3	4	5	6	7	8	9	10	11	average
CO ₂	19.85	14.84	17.06	15.09	18.08	16.27	16.16	18.52	19.87	18.13	14.84	17.15
SO ₃	1.92	2.14	2.66	4.19	3.65	3.10	3.30	2.00	1.99	2.28	1.07	2.57
P ₂ O ₅	0.00	0.00	0.00	0.00	0.00	0.01	0.00	0.00	0.00	0.00	0.00	0.00
SiO ₂	0.06	0.11	0.20	0.36	0.30	0.05	0.05	0.06	0.16	0.07	0.10	0.14
Cl	0.37	0.24	0.35	0.36	0.40	0.22	0.31	0.36	0.32	0.48	0.16	0.32
NiO	67.07	69.61	69.62	69.67	66.74	69.06	70.65	69.00	67.89	68.63	70.66	68.96
MgO	1.58	0.48	0.68	0.85	0.91	1.07	0.96	1.77	0.54	1.46	0.22	0.96
FeO	0.74	0.59	1.19	0.06	0.08	0.00	0.16	0.58	1.29	0.27	0.75	0.52
CoO	0.04	0.00	0.05	0.25	0.14	0.05	0.00	0.00	0.05	0.08	0.12	0.07
CaO	0.24	0.10	0.06	0.04	0.05	0.05	0.05	0.21	0.14	0.23	0.09	0.11
Al ₂ O ₃	0.17	0.01	0.80	0.02	0.02	0.01	0.04	0.05	0.06	0.00	0.04	0.11
CuO	0.00	0.66	1.30	0.00	0.34	0.41	0.00	0.04	1.19	0.04	1.28	0.48
MnO	0.02	0.54	1.61	2.03	1.54	0.04	0.01	0.05	0.46	0.02	0.14	0.59
Total	92.07	89.33	95.57	92.91	92.24	90.34	91.69	92.64	93.95	91.68	89.47	91.99
H ₂ O*	7.93	10.68	4.43	7.09	7.76	9.66	8.31	7.36	6.05	8.32	10.53	8.01

*Calculated by difference to 100 %.

Table 2. EPMA on zaratite particles taken on the dark-green areas of specimens from Heazlewood (Tasmania, Australia) and Texas, Lancaster County (Pennsylvania, USA).

	Texas, Lancaster County (Pennsylvania, USA)								Heazlewood (Tasmania, Australia)							
	1	2	3	4	5	6	7	aver.	1	2	3	4	5	6	7	aver.
CO ₂	34.31	32.19	33.34	36.08	37.44	36.86	35.19	35.06	20.58	17.68	18.05	17.70	18.77	20.65	18.17	18.80
SO ₃	0.66	0.45	0.49	0.55	0.32	0.36	0.27	0.44	0.98	1.24	1.05	1.07	1.12	1.00	1.42	1.13
P ₂ O ₅	0.00	0.01	0.06	0.03	0.03	0.01	0.00	0.02	0.00	0.03	0.05	0.00	0.03	0.01	0.01	0.02
SiO ₂	1.76	3.86	3.37	0.00	0.03	0.01	0.00	1.29	0.00	0.02	0.00	0.00	0.00	0.00	0.00	0.00
Cl	0.09	0.08	0.07	0.04	0.04	0.04	0.04	0.06	0.46	0.45	0.49	0.51	0.49	0.50	0.49	0.48
NiO	60.82	58.36	60.83	57.66	60.99	57.74	55.86	58.89	58.05	57.34	58.69	57.90	56.24	57.05	54.75	57.15
MgO	0.77	0.80	0.78	0.88	0.64	0.67	0.64	0.74	0.00	0.00	0.00	0.00	0.02	0.00	0.01	0.00
FeO	0.08	0.05	0.08	0.03	0.04	0.02	0.00	0.04	0.06	0.06	0.10	0.05	0.00	0.01	0.07	0.05
CoO	0.37	0.34	0.27	0.24	0.19	0.20	0.14	0.25	0.00	0.03	0.00	0.09	0.24	0.17	0.15	0.10
CaO	0.08	0.12	0.14	0.09	0.11	0.12	0.12	0.11	0.00	0.00	0.00	0.00	0.02	0.00	0.00	0.00
Al ₂ O ₃	0.01	0.02	0.05	0.00	0.00	0.00	0.00	0.01	0.11	0.03	0.16	0.11	0.11	0.05	0.11	0.10
CuO	0.02	0.00	0.00	0.00	0.00	0.00	0.00	0.00	1.23	1.00	0.25	0.10	0.00	0.34	0.00	0.42
MnO	0.03	0.08	0.08	0.00	0.00	0.00	0.03	0.03	0.00	0.04	0.02	0.02	0.08	0.02	0.02	0.03
Total	98.99	96.35	99.55	95.58	99.81	96.03	92.30	96.94	81.48	77.90	78.85	77.55	77.10	79.80	75.19	78.27
H ₂ O*	1.01	3.65	0.45	4.42	0.19	3.97	7.70	3.06	18.52	22.10	21.15	22.45	22.90	20.20	24.81	21.73

*Calculated by difference to 100 %.

(ii) the calculation basis was a fixed number (3) of Ni-type cations (Ni, Mg, Cu, Al, Fe, Ca) and these metal cations were charge-balanced by available CO₃, SO₄, SiO₄, Cl and as much OH as needed, (iii) all analyzed elements were included in the chemical formula of the mineral since all spot analyses were carried out on clean micro-fragments of zaratite as observed under the optical microscope and EPMA, avoiding other mineral phases. The average formula obtained for Cape Ortegale material is: Ni_{2.86} Mg_{0.07} Fe_{0.02} Cu_{0.02} Mn_{0.03} (CO₃)_{1.21} (SO₄)_{0.10} (OH)_{3.33} Cl_{0.03}. Table 2 shows two selections of seven EPMA spot analyses each performed on zaratite samples from Pennsylvania and Heazlewood; the average formulae calculated in the same way as for Spanish zaratite are, for Pennsylvania, Ni_{2.91} Mg_{0.07} Co_{0.01} Ca_{0.01} (CO₃)_{2.94} (SO₄)_{0.04} (OH)_{0.03} Cl_{0.01} · 0.61H₂O (SiO₄ was not included to keep the electrical neutrality) and, for Heazlewood, Ni_{2.97} Cu_{0.02} Co_{0.01} (CO₃)_{1.66} (SO₄)_{0.01} (OH)_{2.51} Cl_{0.05} · 3.43H₂O.

3.2. ESEM-EDS analyses

The whole type-specimen of zaratite from Cape Ortegale was placed in the ESEM chamber with the aim of studying the best zaratite-rich area. Such an area is shown in Fig. 2a on which the host rock of grey colour and the paragenetic magnesium carbonates of white colour can also be observed. The picture in Fig. 2b was taken from a little pale-green area using the backscattering ESEM probe. Figure 2d and 2e correspond to the *emerald*-green zaratite-rich fragments. The ESEM survey shows different minerals, habits and associations for which the following chemical-mineralogy can be inferred (Fig. 2c): (1) NiCO₃ rich area, with accessory MgCO₃, FeCO₃, and NiSO₄; (2) MgCO₃-rich area with NiCO₃ and NiSO₄; (3) NiCO₃-rich area with NiSO₄ and MgCO₃; (4) NiCO₃ with NiSO₄, MgCO₃ and host rock (possible serpentine); (5) fibrous

MgCO₃ with NiCO₃ and NiSO₄, (6) NiCO₃, CaCO₃ and MgCO₃ impurities. These EDS elemental analyses were performed along with the paragenesis to evidence the considerable chemical variability into the specimen. They provide an excellent view of the sample but these EDS elemental analyses are different and less accurate than the chemical analyses provided by the EPMA technique.

3.3. X-ray diffraction

The X-ray diffraction patterns (Fig. 3) of zaratite can be interpreted as those of low-crystallinity material together with accessory peaks spiking above the amorphous XRD band. In accordance with the structural study of other zaratite samples (Isaacs, 1963), they cannot be indexed with a cubic cell. We also explored the possible presence of accessory minerals using XPOWDER software (www.xpowder.com) performing background subtraction, K α_2 stripping and chemical elements restrained to Ni, Fe, Cu, Si, Pb, Mg and C. These initial features improve the Boolean search-matching on the ICDD-PDF2 and RRUFF databases suggesting some PDF2 card files, as follows: magnesite 86–2348 (peak 2.759 Å), magnetite 86–1352 (peak 2.548 Å), galena 78–1055 (peak 2.959 Å), and other unidentified species with maximum intensities at 2.637 and 1.745 Å. These minerals are compatible with the Cape Ortegale parageneses of serpentine, schist and ultramafic mineralizations. The type specimen of zaratite from Cape Ortegale is a thin patina of *emerald*-green colour covering a metallic massive rock which was also analyzed by XRD. The XPOWDER software analysis of the XRD profile shows the following semi-quantitative mineralogical analysis for the Cape Ortegale host rock: 35 % antigorite (card 21–0963), 44 % hematite (21–0599), 18 % magnetite (21–2315), 3 % global low-crystallinity components. Density = 4.299 g/cm³ and μ/Dx of the mixture = 156.1

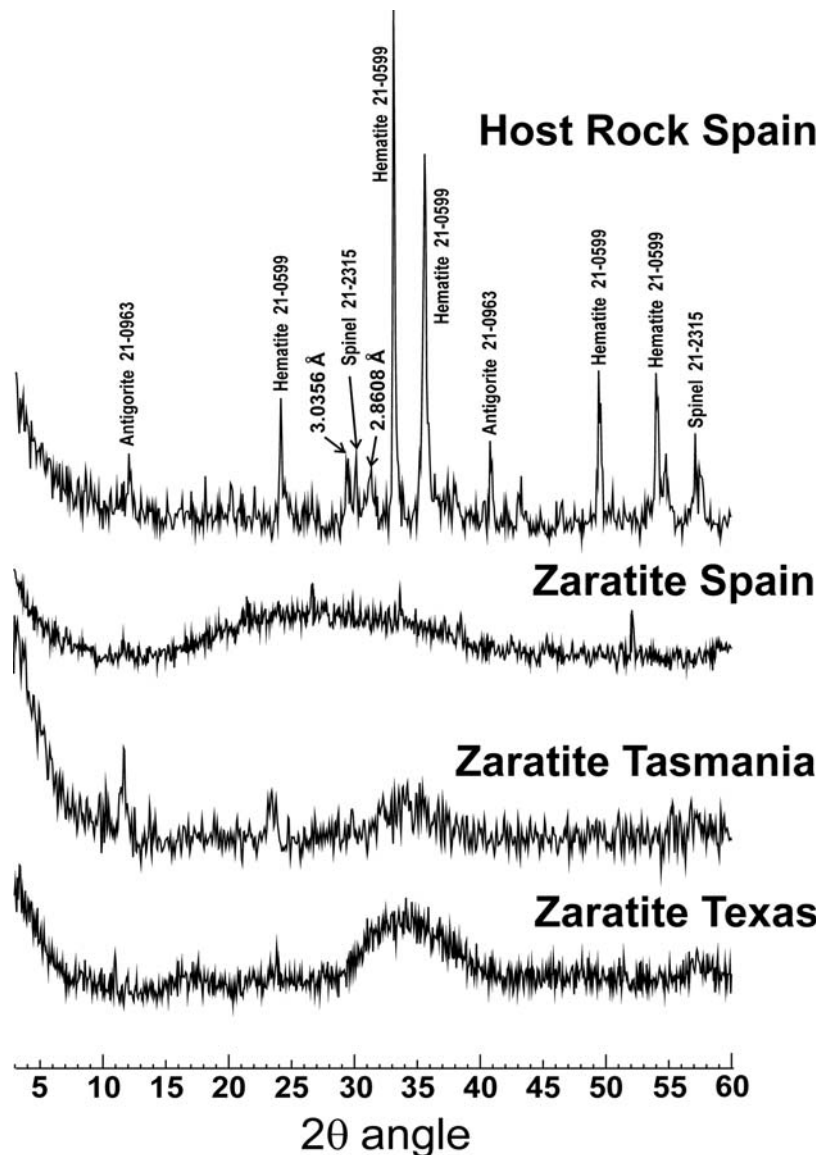


Fig. 3. X-ray diffraction analysis. Top.- Host-rock XRD pattern displaying main lines of spinel-magnetite, hematite, serpentine-antigorite and characteristic lines of carbonates at 3.03 and 2.86 Å. Bottom.- XRD patterns of zaratite emerald-green fragments from Cape Ortegale, Tasmania and Pennsylvania, showing a low crystallinity with different minor impurities.

cm²/g. Concerning the other specimens of zaratite used for comparison: (i) The Tasmania powdered translucent green layer displays an XRD profile typical of a low degree of crystallinity with accessory peaks at 7.26, 3.62 Å, *etc.*, assigned to lizardite (72–1500). In addition, XRD analysis of the powdered host rock with the Xpovder software suggests 75 % of lizardite (50–1606) and 25 % of chlorite (50–0025). (ii) The Pennsylvania powdered green layer shows also a low-crystallinity XRD profile with accessory peaks of possible jamborite (89–7111), stichtite (89–1475) and pyroaurite (89–0521); for the powdered host-rock sample the Xpovder software yields 62 % antigorite (21–0963), 22 % clinocllore (82–0038), 14 % sjoegrenite (86–0182) and 2 % magnesite (86–0175).

3.4. DTA-TG analyses

Figure 4 shows the TG and DTA results of the type specimen of zaratite from Cape Ortegale. The DTA curve shows an endothermic peak at *ca.* 280 °C and a TG slope from 230 °C to 350 °C (~17 wt%) attributed to the release of hydroxyl and CO₂ groups. Above this temperature, from 600 °C up to 650 °C a considerable weight loss is observed (~10 %) which can be attributed to CO₂ release. The DTA variations observed at *ca.* 650 °C can be explained by the whole thermal decomposition of the carbonate followed by crystallization of nickel oxide. Specimens Pennsylvania and Heazlewood do not provide good enough DTA-TG analyses by scarcity of pure samples.

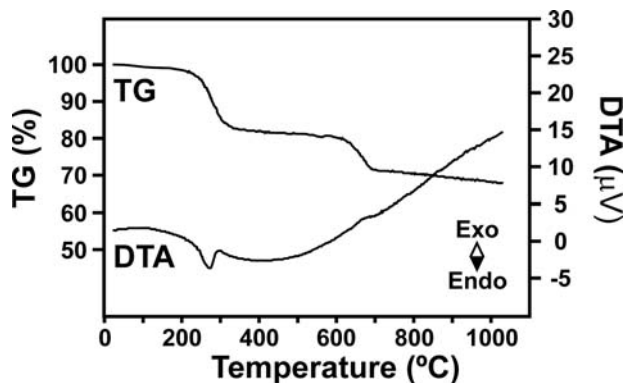


Fig. 4. Differential-thermal and thermo-gravimetric analyses of the type specimen of zaratite from Cape Ortegá (Coruña, Spain).

3.5. Raman spectra

The main bands of the Raman spectrum of the type specimen of zaratite from Ortegá Cape occur at 458, 536, 788, 941, 982, 1073, 1366 and 1609 cm^{-1} (Fig. 5a). In accordance with Frost *et al.* (2008): (i) the band at 458 cm^{-1} may be assigned to the NiO stretching vibration, (ii) the broad

minor band with peaks at 685 and 780 cm^{-1} may be assigned to CO_3^{2-} ν_4 bending modes; (iii) the 941 and 982 cm^{-1} peaks are generally attributed to OH deformation vibration modes in agreement with FTIR data on Heazlewood zaratite obtained by the same authors; (iv) the 1073 cm^{-1} and 1366 cm^{-1} peaks are associated with ν_1 symmetric and ν_3 antisymmetric stretching vibration modes of the carbonate anion and finally (v) the visible band at 1609 cm^{-1} can be attributed to water bending mode. Figure 5b shows the Raman spectrum of a neighbouring spot recorded with the extended grating to observe the longer Raman shift region exhibiting: (1) a group of peaks at 2935, 2867 and 2753 cm^{-1} attributed to organic molecules on the mineral surface, and (2) an other group at 3110, 3217, 3328, 3428 and 3604 cm^{-1} assigned to OH stretching vibrations.

Figure 6a displays comparative Raman spectra from 200 to 3000 cm^{-1} of the three zaratite specimens, exhibiting similarities in the spectral positions with some differences in peak intensities. The Tasmanian specimen displays the broad band from 685 and 780 cm^{-1} assigned to CO_3^{2-} ν_4 bending modes including a detached large peak at 842 cm^{-1} . The three zaratite specimens show large Raman peaks at 941, 982, 1073 and 1366 cm^{-1} with minor differences among each other.

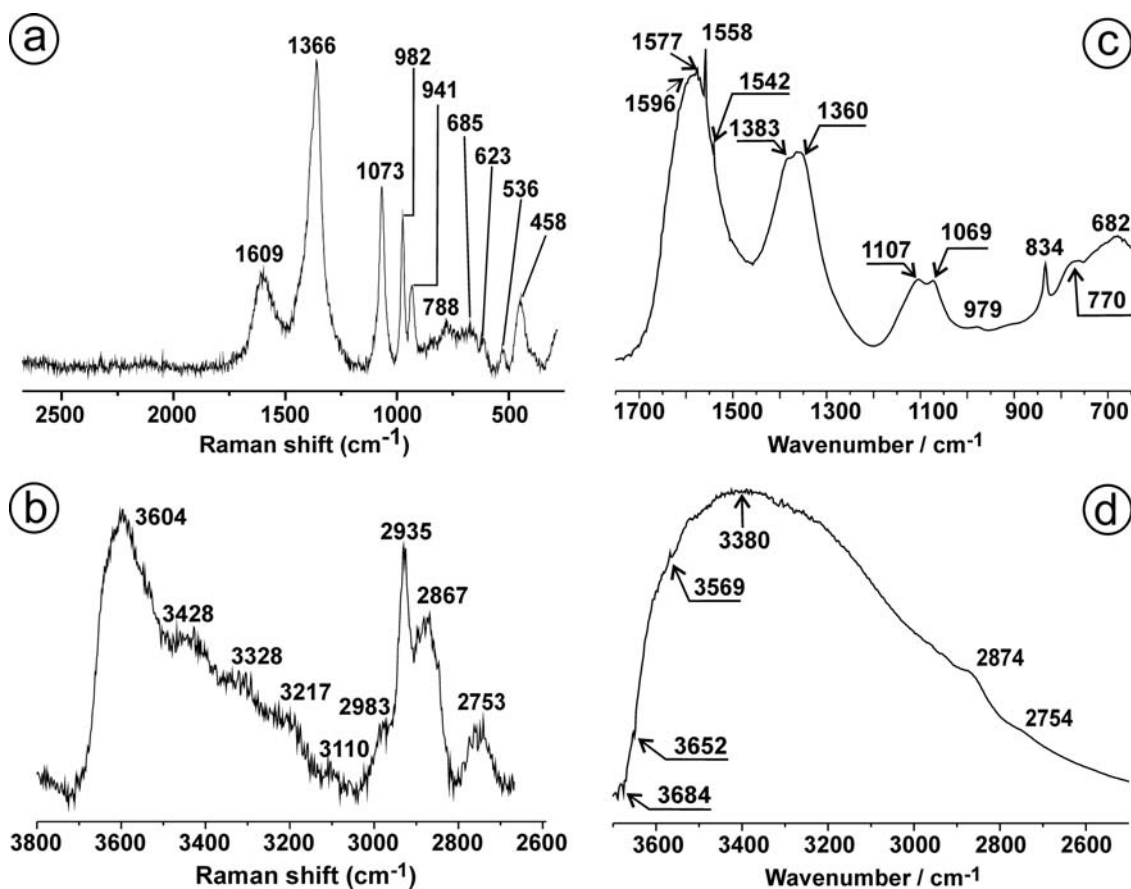


Fig. 5. Raman and FTIR analyses of zaratite from Cape Ortegá with focus on the main spectral areas and peaks: (a) Raman 500–2500 cm^{-1} region, (b) Raman 2600–3800 cm^{-1} region, (c) FTIR 700–1700 cm^{-1} region, (d) FTIR 2500–3700 cm^{-1} region.

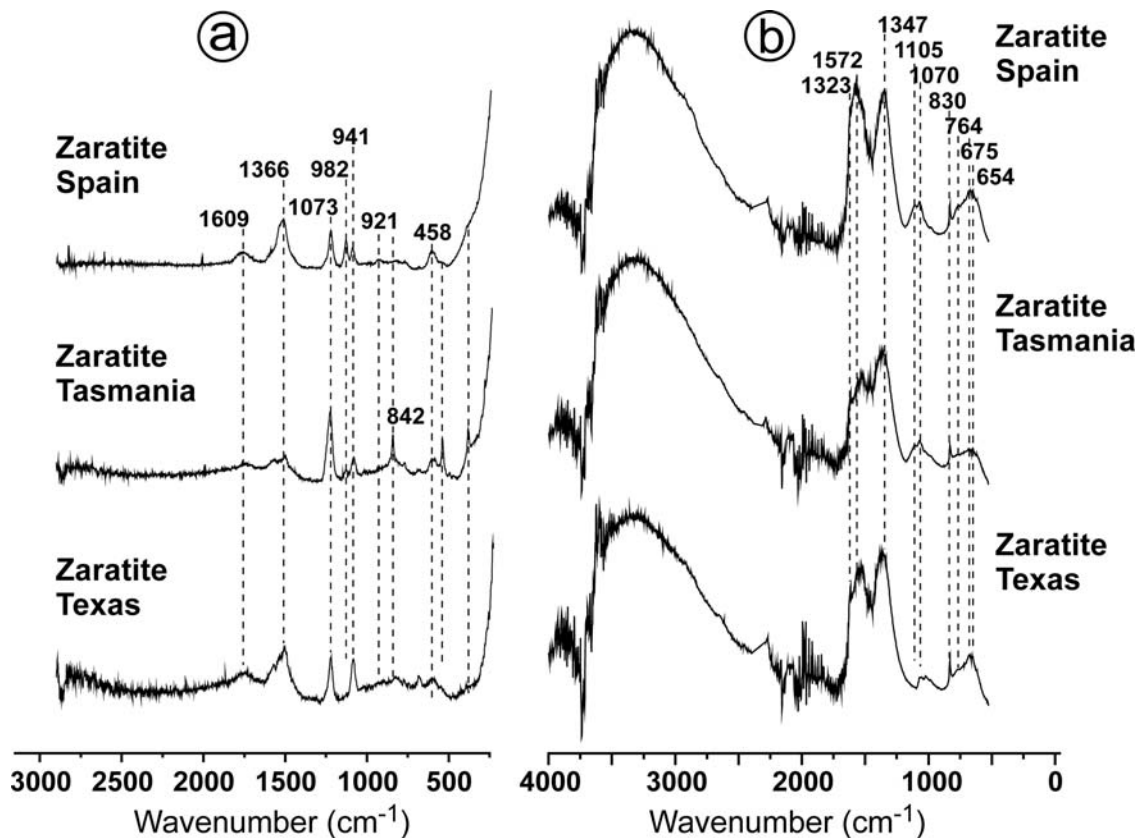


Fig. 6. Comparative (a) Raman and (b) FTIR spectra for the three zaratite samples analyzed from Cape Ortegale (Spain), Heazlewood (Tasmania) and Texas, Lancaster County (Pennsylvania).

3.6. FTIR spectra

The type specimen from Ortegale Cape shows an FTIR spectrum with the following features: (i) a main band with accessory peaks at 1596, 1577, 1558, 1542, 1383 and 1360 cm^{-1} associated to hydroxyl and water molecular groups in nickel carbonate minerals (Fig. 5c); (ii) two coupled peaks at 1360 cm^{-1} and 1383 cm^{-1} usually attributed to CO_3^{2-} ν_3 antisymmetric stretching vibrations; (iii) a band peaked at 1069 and 1107 cm^{-1} associated with OH groups; (iv) a detached peak at 834 cm^{-1} assigned to the CO_3^{2-} ν_2 bending mode and (v) bands at 682 and 770 cm^{-1} could be assigned to the CO_3^{2-} ν_4 in-phase bending mode. In the infrared spectrum at shorter wavelengths (Fig. 5d) the broad region of bands peaked at 3380 and 3569 cm^{-1} is commonly assigned to water stretching vibrations while the FTIR band at 2874 cm^{-1} could be associated with C–H stretching due to adsorbed organic molecules. Figure 6b displays a comparison of the FTIR spectral curves of the three zaratite specimens, with no noticeable difference between them.

4. Discussion

The three zaratite specimens match with the mineralogical card-file of zaratite in the Handbook of Mineralogy

(Anthony *et al.*, 2003, <http://www.handbookofmineralogy.org/>) for zaratite from various localities, which states the following information: (i) Crystal Data: coatings composed by spherulitic masses and gel-like low-crystallinity materials, (ii) Physical properties: conchoidal fracture, $H = 3.5$, (iii) Optical properties: isotropic, translucent, colour *emerald-green*, green in transmitted light, luster vitreous to greasy, (iv) Cell data not determined from a semi-amorphous or low-crystallinity XRD pattern, (v) Chemistry variable, (vi) Occurrence as secondary mineral formed by alteration of pentlandite, pyrrhotite, and millerite in serpentinites and ultramafic rocks, and (vii) Association with calcite, dolomite and magnesite. This set of features has been the main reason to maintain the use of the zaratite term to name this type of materials.

Micro-samples of zaratite from Cape Ortegale, Tasmania and Pennsylvania were analyzed by EPMA. The accuracy of the C measurements by this technique is low despite being operated in the best experimental conditions, *i.e.*, acceleration voltage 15 kV, probe current 20 nA, 10 μm beam. These measurements could include 5 % error. Taking into account that the % H_2O was obtained by difference to 100 %, the associated errors could even be greater than 5 %. The EPMA carbon values cannot be considered as absolute values. However, they should allow comparison of the three samples analyzed under the same conditions. The average formula of the type

specimen of zaratite from Cape Ortegale can be written as: $\text{Ni}_{2.86}\text{Mg}_{0.07}\text{Fe}_{0.02}\text{Cu}_{0.02}\text{Mn}_{0.03}(\text{CO}_3)_{1.21}(\text{SO}_4)_{0.10}(\text{OH})_{3.33}\text{Cl}_{0.03}$ while those for zaratite samples from Pennsylvania and Tasmania are $\text{Ni}_{2.91}\text{Mg}_{0.07}\text{Co}_{0.01}\text{Ca}_{0.01}(\text{CO}_3)_{2.94}(\text{SO}_4)_{0.04}(\text{OH})_{0.03}\text{Cl}_{0.01} \cdot 0.61\text{H}_2\text{O}$ and $\text{Ni}_{2.97}\text{Cu}_{0.02}\text{Co}_{0.01}(\text{CO}_3)_{1.66}(\text{SO}_4)_{0.01}(\text{OH})_{2.51}\text{Cl}_{0.05} \cdot 3.43\text{H}_2\text{O}$, respectively. The comparison of these formulae can be made through the molar ratios Ni/CO₃, Ni/OH and H₂O/Ni, as follows: Cape Ortegale (2.37; 0.86; 0), Tasmania (1.79; 1.18; 1.15), and Pennsylvania (0.99; 111.80; 0.21). Clearly, natural nickel hydroxycarbonate hydrate materials, collectively referred to as ‘zaratite’, are chemically distinct, resembling either anhydrous zaratite (Ortegale), nullagine (Tasmania), or gaspéite (Pennsylvania). From the crystal-chemical point of view, natural zaratites are far away from the theoretical zaratite formula accepted in the literature, *i.e.*, $\text{Ni}_3\text{CO}_3(\text{OH})_4 \cdot 4\text{H}_2\text{O}$.

The X-ray diffraction patterns of these three samples, shown in Fig. 3, were obtained from three powdered apparently pure, translucent and emerald-green colour fragments. All of them show the typical features of the low-crystallinity substances. In addition, these clean materials typically produce accessory peaks attributable to paragenetic minerals, also detected in the host rocks.

The thermal behaviour of the Cape Ortegale zaratite sample is characteristic of anhydrous nickel hydroxycarbonate. The assumption is supported by the fact that the DTA curve does not show peaks in the 110 °C–120 °C interval attributed to water molecules loss by Fried & Dollimore (1994) in synthetic $\text{Ni}_3\text{CO}_3(\text{OH})_4 \cdot 4\text{H}_2\text{O}$. The endothermic peak at *ca.* 280 °C is clearly observed together with the strong TG slope in the range 230 °C to 350 °C, which can be attributed to the release of hydroxyl and CO₂ groups and the formation of nickel oxide as suggested in previous papers (*e.g.*, Henmi *et al.*, 1986; Fried & Dollimore, 1994; Shaheen, 2002). The sum of both TG losses, *i.e.*, from 230 °C to 350 °C (~17 %) and from 600 °C up to 650 °C (~10 %) is 27 %. This value is in good agreement with those obtained by EPMA (25.2 %). The small DTA-TG features observed at *ca.* 650 °C can be explained by whole CO₂ release and recrystallization of NiO (Mallaya & Vasudeva-Murthy, 1961; Uzunova *et al.*, 1994). Small energy changes by re-crystallization and densification of NiO, not detected in the DTA spectrum, occur at temperatures higher than 700 °C (Rhamdhani *et al.*, 2008). These DTA-TG results match well with the phase $\text{Ni}_3\text{CO}_3(\text{OH})_4$, which is not known as a mineral but which could be easily formed by dehydration from zaratite placed in dry-warm environments.

The Raman peak assignments demonstrate the existence of anion groups CO₃²⁻, SO₄²⁻, OH⁻, of Ni–O stretching vibrations and water bending modes. The Raman spectrum recorded on the Spanish zaratite matches well with both Heazlewood and Pennsylvania zaratite spectra. The FTIR bands observed in the ~1600 to ~1300 cm⁻¹ spectral region are associated with both hydroxyl groups and water molecules in carbonates (Huang & Kerr, 1960) (Fig. 5c). Following Huang & Kerr (1960) the main infrared peak at 1546 cm⁻¹ can be attributed to the Ni–CO₃

groups by comparison with the infrared spectra of anhydrous rhombohedral (calcite) and orthorhombic (aragonite) carbonates. The two spectral shoulders at 1639 and 1430 cm⁻¹ could be explained by comparison with the spectra of carbonates containing hydroxyl or halogen components. That sample of zaratite collected in the humid cliffs of Cape Ortegale was very probably a fully hydrated specimen in 1850. This assumption is supported by the humid environment of the outcrops and by the original water estimation of Casares described by Martinez Alcibar (1850): ‘‘copious yield of water in the closed tube’’. At present the three zaratite specimens, *i.e.*, Ortegale, Pennsylvania and Heazlewood, exhibit similar naked-eye properties, structure and colour of thin emerald-green translucent patinas on the host rocks. In the same way, the XRD, Raman and FTIR spectra of the three zaratite specimens show minor differences between them.

5. Conclusions

- (i) The EPMA series performed on the three zaratite samples reveal different chemical compositions. The mineralogical formulae exhibit different molar ratios (Ni/CO₃, Ni/OH and H₂O/Ni), as follows: Ortegale (2.37; 0.86; 0), Heazlewood (1.79; 1.18; 1.15), and Pennsylvania (0.99; 111.80; 0.21), suggesting that the natural nickel hydroxycarbonate hydrate materials collectively referred to as ‘zaratite’ are chemically distinct, resembling either anhydrous zaratite (Cape Ortegale), nullagine (Tasmania) or gaspéite (Pennsylvania). Accordingly, the formulae calculated for the three specimens differ from each other and from the zaratite formula commonly reported in databases, *i.e.*, $\text{Ni}_3\text{CO}_3(\text{OH})_4 \cdot 4\text{H}_2\text{O}$.
- (ii) The XRD patterns of the three international ‘‘zaratite samples’’ only validate their low-crystallinity character, with variable mineral inclusions.
- (iii) The thermal behaviour of the Ortegale zaratite sample is characteristic of anhydrous nickel hydroxycarbonate $\text{Ni}_3\text{CO}_3(\text{OH})_4$, unknown as a mineral phase but which could be easily formed by dehydration from hydrated zaratite placed in dry-warm environments.
- (iv) The Raman and FTIR spectra display large similarities among the three samples. In the absence of long-range order (XRD), the similarity of the spectra obtained with these short-range probes on the different samples is no argument for a single species status; it just confirms the general chemical kinship of these materials.
- (v) These facts confirm the former reservations expressed by Isaacs (1963) concerning the zaratite mineral status and the Q (questionable) assigned by the IMA to zaratite. Our data suggest that the natural nickel hydroxycarbonate materials, collectively referred to as ‘zaratite’ on the basis of colour, occurrence and poor crystallinity, are in fact so diverse in terms of Ni/C/H ratios that ‘zaratite’ should not

deserve a species status and so remains highly questionable. At best, this name could be further used (within quotes) for practical purposes to designate such natural material, without implication as to a species name.

Acknowledgements: We are grateful to the Spanish project CGL2010-17108 and the CSIC Institution.

References

- Anderson, P., Bottrill, R., Davidson, P. (2002): The Lord Brassey mine, Tasmania. *Mineral. Rec.*, **33**(4), 321–332.
- Anthony, J.W., Bideaux, R.A., Bladh, K.W., Nichols, M.C. (2003): Handbook of Mineralogy, Mineralogical Society of America, Chantilly, VA 20151–1110, USA. <http://www.handbookofmineralogy.org/>.
- Fenoglio, M. (1934): Sulla struttura cristallina della zaratite. *Per. Miner. Roma*, **5**, 33–36.
- Fried, D. & Dollimore, D. (1994): Isothermal and rising temperature kinetic studies of doped non-stoichiometric basic nickel carbonate. *J. Therm. Anal.*, **41**, 323–336.
- Frost, R.L., Dickfos, M.J., Reddy, B. (2008): Raman spectroscopy of hydroxy nickel carbonate minerals nullaginite and zaratite. *J. Raman Spectr.*, **39**, 1250–1256.
- Frost, R.L., Keeffe, E.C., Reddy, B.J. (2010): Characterisation of Ni carbonate-bearing minerals by UV-Vis-NIR spectroscopy. *Transit. Metal Chem.*, **35**, 279–287.
- Henmi, H., Mori, M., Hirayama, T. (1986): Influence of the self-generated and controlled atmosphere on the thermal decomposition of basic nickel carbonate, $\text{NiCO}_3 \cdot 2\text{Ni}(\text{OH})_2 \cdot 4\text{H}_2\text{O}$. *Thermochim. Acta*, **104**, 101–109.
- Huang, C.K. & Kerr, P.F. (1960): Infrared study of the carbonate minerals. *Am. Mineral.*, **45**, 311–324.
- Isaacs, T. (1963): The mineralogy and chemistry of nickel carbonates. *Mineral. Mag.*, **33**, 663–678.
- Mallaya, R.M. & Vasudeva-Murthy, A.R. (1961): Studies on the basic carbonates of nickel. *J. Indian Inst. Sci.*, **43**, 65–130.
- Martinez Alcibar, A. (1850): Raro e importante mineral de niquel. *Rev. Minera Madrid*, **10**, 302–306.
- Rhamdhani, M.A., Jak, E., Hayes, P.C. (2008): Basic nickel carbonate, Part II microstructure evolution during industrial nickel production from basic nickel carbonate. *Metal. Mater. Trans. B*, **39**, 234–245.
- Shaheen, W.M. (2002): Thermal behavior of pure and binary basic nickel carbonate and ammonium molybdate systems. *Mater. Lett.*, **52**, 272–282.
- Smith, J.L. & Brush, G.J. (1853): Reexamination of American minerals. *Am. J. Sci.*, **41**, 365–373.
- Uzunova, E., Klissurski, D., Kassabov, S. (1994): Nickel-iron hydroxide carbonate precursors in the synthesis of high-dispersity oxides. *J. Mater. Chem.*, **4**, 153–159.
- Williams, K.L., Threadgold, I.M., Hounslow, A.W. (1959): Hellyerite, a new nickel carbonate from Heazlewood, Tasmania. *Am. Mineral.*, **44**, 533–538.

Received 8 November 2012

Modified version received 9 June 2013

Accepted 30 June 2013